2 Exotic Higgs phenomenology from S_3 flavor symmetry

***G. Bhattacharyya*, P. Leser, H. Päs**

Abstract We consider an S_3 flavor symmetry model, and by imposing this global discrete symmetry in the scalar potential we observe some interesting decay signatures of a light scalar and a pseudo-scalar which might be buried in the existing collider data.

2.1 Introduction

Discrete flavor symmetries are often used to explain the masses and mixing of quarks and leptons [1–4]. These scenarios predict nonstandard decay signatures involving scalars and gauge bosons, and flavor changing neutral currents (FCNC). The flavor group S_3 was introduced early in Ref. [5] and has since been used in many different scenarios [6–16]. Our analysis is based on the realization in Ref. [17]. The group structure of S_3 favors maximal atmospheric mixing angle which still gives a good fit after the recent measurements of non-zero θ_{13} [18–20]. S_3 has three irreducible representations: $\mathbf{1}, \mathbf{1}'$, and $\mathbf{2}$. The invariants $\mathbf{1}$ can be constructed using the multiplication rules $\mathbf{2} \otimes \mathbf{2} = \mathbf{1} \oplus \mathbf{1}' \oplus \mathbf{2}$ and $\mathbf{1}' \otimes \mathbf{1}' = \mathbf{1}$. We take the particle assignments [17], which we have followed also in Ref. [21, 22]:

$$\begin{aligned}
&(L_\mu, L_\tau) \in \mathbf{2}\,, && L_e, e^c, \mu^c \in \mathbf{1}\,, && \tau^c \in \mathbf{1}'\,, \\
&(Q_2, Q_3) \in \mathbf{2}\,, && Q_1, u^c, c^c, d^c, s^c \in \mathbf{1}\,, && b^c, t^c \in \mathbf{1}'\,, \\
&(\phi_1, \phi_2) \in \mathbf{2}\,, && \phi_3 \in \mathbf{1}\,.
\end{aligned} \tag{2.1}$$

The fields $Q_{1/2/3}$ and $L_{e/\mu/\tau}$ are the quark and lepton $SU(2)$ doublets of the three generations. This assignment was motivated in Ref. [17] to have a reasonably successful reproduction of quark and lepton masses and mixing. All the three scalar $SU(2)$ doublets $\phi_{\{1,2,3\}}$ take part in electroweak symmetry breaking. The general structure of the model allows for tree-level FCNC due to the absence of natural flavor conservation [23], although those are too suppressed by the Yukawa couplings to cause any problem even for scalar masses of the electroweak scale [21, 22, 24]. However, in models where the flavor symmetry does not apply on Yukawa couplings, the scalar masses are pushed beyond the TeV scale [25]. In our analysis [21, 22] we observe noteworthy decay properties of a scalar and a pseudo-scalar: (*i*) Two of the three scalars $h_{b,c}$ have standard model (SM)-like gauge and Yukawa couplings, and they can dominantly decay into the third absolutely non-SM-like scalar h_a; (*ii*) The scalar (pseudo-scalar) h_a (χ_a) has no $(h_a/\chi_a)VV$-type vertices, where $V \equiv W^\pm, Z$; (*iii*) h_a/χ_a has *only* flavor off-diagonal Yukawa couplings with one fermion from the third generation. We have included all scalar degrees of freedom: three CP-even neutral scalars, two CP-odd neutral scalars and two sets of charged scalars. The special features of our analysis are: (i) determination of the mass spectrum of the neutral scalars/pseudoscalars and the charged scalars following an improved potential minimization method, (ii) calculation of their gauge and Yukawa couplings, and (iii) identification of a novel decay channel of a scalar (pseudoscalar) which can be experimentally tested.

2.2 Mass spectrum

The explicit form of the general S_3 invariant scalar potential, which we do not give here for brevity, is given in Refs. [21, 22, 26]. It has eight dimensionless couplings λ_i and two mass-squared dimensional parameters m^2 and m_3^2.

The replacement $\phi_i \to \left(h_i^+, v_i + h_i + \mathrm{i}\chi_i\right)^{\mathsf{T}}$ is done, assuming $v_1 = v_2 = v$ and v_3, which allow for maximal atmospheric neutrino mixing, where $2v^2 + v_3^2 = v_{\rm SM}^2$ has to hold with $v_{\rm SM} = 246\,\text{GeV}$. After diagonalizing the mass matrices the physical CP-even, CP-odd and charged scalars are denoted by $h_{a,b,c}$, $\chi_{a,b}$ and $h_{a,b}^+$, respectively.

Note that by imposing $v_1 = v_2$ on the potential m^2 and m_3^2 are related to the couplings λ_i and the VEVs v and v_3. To make sure that this point is actually a minimum of the potential, the determinant of the Hessian has to be positive, which is equivalent to imposing the condition of positive squared scalar masses. As a first step towards potential minimization, we first try to provide an analytical feel. We identify some simple-looking relations of the coefficients that keep the potential always bounded from below. To do this we factorize the scalar potential into a simplified polynomial in ϕ_1, ϕ_2 and ϕ_3. Three distinct types of terms emerge with power four: ϕ_i^4, $\phi_i^2\phi_j^2$ and $\phi_i^2\phi_j\phi_k$, where $i, j, k = 1\dots 3$. Of the nine terms, only six have independent coefficients, which we call $c_{\{1\dots 6\}}$:

$$c_1\phi_1^4 + c_1\phi_2^4 + c_2\phi_3^4 + c_3\phi_1^2\phi_2^2 + c_4\phi_1^2\phi_3^2 + c_4\phi_2^2\phi_3^2 + c_5\phi_1^2\phi_2\phi_3 + c_5\phi_1\phi_2^2\phi_3 + c_6\phi_1\phi_2\phi_3^2\,. \tag{2.2}$$

It follows that

$$c_1 = \lambda_1/2 + \lambda_2/2, \quad c_2 = \lambda_4/2, \quad c_3 = \lambda_1 - \lambda_2 + \lambda_3, \quad c_4 = \lambda_5 + \lambda_6, \quad c_5 = 2\lambda_8, \quad c_6 = 2\lambda_7\,. \tag{2.3}$$

By inspection, the following conditions emerge:

$$\begin{aligned} &c_1, c_2 > 0, \qquad 2c_3, 2c_4 \geq -c_1, \qquad 2c_3, 2c_4 \geq -c_2, \quad 2c_4 \geq -c_1, , \\ &-1/2c_1 \leq c_5, c_6 \leq c_1, \quad -1/2c_2 \leq c_5, c_6 \leq c_2\,. \end{aligned} \tag{2.4}$$

Then we get an acceptable mass spectrum for all types of scalars, and the potential turns out to be globally stable. However, this method overlooks a large part of the otherwise valid parameter, and an uncomfortable feature is that none of the masses exceeds 300 GeV when $\left|\lambda_{\{1\dots 8\}}\right| \leq \pi$.

Now we propose a better method for ensuring global stability. We transform Eq. (2.2) into spherical coordinates (ρ, θ, ϕ), which splits the potential into a radial and an angular part.

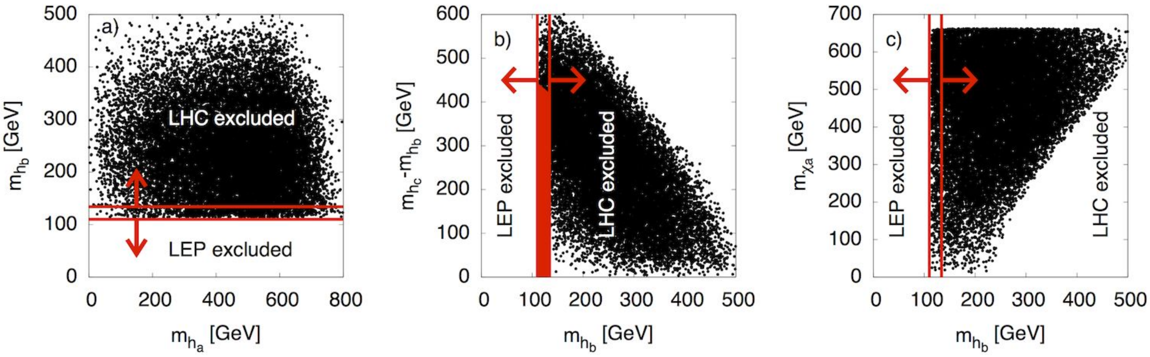

Figure 2.1: *Scatter plots of masses of h_a, h_b, h_c and χ_a, fixing $v_3/v = 0.6$. The lines give the window between $114 - 130$ GeV. The highlighted strip in the middle plot is disfavored by LHC which disfavors a second SM-like Higgs within 550 GeV.*

Global stability then means the positivity of the angular part:

$$\sin^4\theta\{(2c_1-c_3)\cos(4\phi)+6c_1+c_3\}+8c_2\cos^4\theta+\sin^2(2\theta)(2c_4\sin^2\phi+c_6\sin(2\phi)) + 8c_4\cos^2\phi\sin^2\theta\cos^2\theta + 4c_5\sin(2\phi)\sin^3\theta\cos\theta(\sin\phi+\cos\phi) > 0 \quad (2.5)$$

As it is a transcendental inequality, no simple-looking analytic solutions emerge by solving Eq. (2.5). We therefore check the positivity of this function numerically at each point of the parameter space. This method allows us to explore the so-far inaccessible territory of the stable parameter space that could not be reached by Eq. (2.4). Interestingly, the heavy scalar and pseudoscalar masses can be pushed well above 300 GeV even for $\left|\lambda_{\{1\ldots8\}}\right| \leq \pi$.

We express the physical pseudo-scalar (χ) and scalar (h) states denoted by *roman alphabets* as subscripts in terms of their weak eigenstates distinguished by *hindu numerals*:

$$\begin{aligned} &\chi_{1(2)} = (v/v_{\rm SM})\,G^0 \mp \left(1/\sqrt{2}\right)\chi_a - v_3/\left(\sqrt{2}v_{\rm SM}\right)\chi_b, \quad \chi_3 = (v/v_{\rm SM})\,G^0 + \sqrt{2}\,(v_3/v_{\rm SM})\,\chi_b\,; \\ &h_{1(2)} = U_{1(2)b}\,h_b + U_{1(2)c}\,h_c \mp \left(1/\sqrt{2}\right)\,h_a, \qquad h_3 = U_{3b}\,h_b + U_{3c}\,h_c\,, \end{aligned} \quad (2.6)$$

where U_{ib} and U_{ic} are complicated functions of the $\lambda_{\{1\ldots8\}}$, v and v_3. The corresponding mixing relations for $h^+_{a,b}$ are obtained by substituting $\chi \to h^+$ and $G^0 \to G^+$ in Eq. (2.6). The masses for the CP-even scalars are [21, 22]

$$\begin{aligned} m^2_{h_a} &= 4\lambda_2 v^2 - 2\lambda_3 v^2 - v_3\,(2\lambda_7 v_3 + 5\lambda_8 v)\,, \\ m^2_{h_{b(c)}} &= \frac{1}{2v_3}\left[4\lambda_1 v^2 v_3 + 2\lambda_3 v^2 v_3 + 2\lambda_4 v_3^3 - 2\lambda_8 v^3 + 3\lambda_8 v v_3^2 \mp \Delta m^3\right], \end{aligned} \quad (2.7)$$

where Δm^3 is a complicated expression of the λ_i and the VEVs given in Refs. [21, 22].

The pseudo-scalar squared masses are

$$m^2_{\chi_a} = -9\lambda_8 v v_3, \quad m^2_{\chi_b} = -v^2_{\rm SM}\,(2\lambda_7 + \lambda_8 v/v_3)\,, \quad (2.8)$$

while the charged scalars' squared masses are

$$m^2_{h_a^+} = -2\lambda_3 v^2 - v_3^2(\lambda_6 + \lambda_7) + 5\lambda_8 v v_3, \quad m^2_{h_b^+} = -v^2_{\text{SM}}(\lambda_6 + \lambda_7 + \lambda_8 v/v_3)\,. \tag{2.9}$$

The allowed ranges for the masses obtained by varying $\lambda_{\{1...8\}} \in [-\pi, \pi]$ and keeping the ratio v_3/v fixed to 0.6 (chosen in Ref. [21, 22] for compatibility with the quark masses) are shown in Fig. 1. In view of the recent LHC results [27, 28] that claims discovery of a Higgs-like boson at around 125 GeV with a large excluded region above and below, the mass spectrum in this model fits well with the following scenario:

1. h_b is identified with the 125 GeV Higgs boson [27, 28]. The Yukawa and gauge couplings of h_b and h_c are like those of the SM Higgs. h_c is somewhat heavier than h_b.
2. h_a and χ_a have nonstandard interactions that hide them from standard searches.
3. All other masses, including the charged scalars, can be above 550 GeV, although from the experimental point of view the charged scalars need not be that heavy.

2.3 Couplings

	$\mathbf{h_a^\pm W^\mp}$	$\mathbf{h_b^\pm W^\mp}$	$\chi_\mathbf{a}\mathbf{Z}$	$\chi_\mathbf{b}\mathbf{Z}$	$\mathbf{W^\pm W^\mp}$	$\mathbf{ZZ}$
$\mathbf{h_a}$	✓	–	✓	–	–	–
$\mathbf{h_b}$	–	✓	–	✓	✓	✓
$\mathbf{h_c}$	–	✓	–	✓	✓	✓

	$\mathbf{h_a^\pm W^\mp}$	$\mathbf{h_b^\pm W^\mp}$
$\chi_\mathbf{a}$	✓	–
$\chi_\mathbf{b}$	–	✓

Table 2.1: *3-point vertices with at least one h (or χ) and W/Z boson. A checkmark means that the vertex exists.*

The couplings involving h_a do not depend on the scalar potential parameters, while those of of h_b and h_c do and that too in a complicated way, which we refer by putting checkmark signs in Tables 2.1 and 2.2 without displaying their expressions explicitly. The $h_a\chi_a Z$ coupling is $\frac{i}{2}Gq_\mu$, where $G = \sqrt{g^2 + g'^2}$ and q_μ is the momentum transfer. Since neither h_a nor χ_a couples to pairs of gauge bosons via the three-point vertex, their masses are not constrained from direct searches at LEP2 or by electroweak precision tests. In fact, the conventional LHC Higgs search strategy would not apply on them either. Now we come to Yukawa interaction, whose explicit form is given in Refs. [21, 22].

The scalars are rotated to their physical basis $\{h_a, h_b, h_c\}$, and we obtain the Yukawa matrices $Y_{\{a,b,c\}}$. The individual mixing matrices for up- and down-type quarks contain large mixing angles as a consequence of S_3 symmetry and the particle assignments [17]. Specifically, the doublet representation of S_3 generates maximal mixing when we set $v_1 = v_2$. Now, the CKM matrix involves a relative alignment of those two matrices which yields small mixing for quarks. Similarly, the PMNS matrix is given by the relative orientation of the mixing matrices for the charged leptons and neutrinos. Since we assume that the neutrino mass matrix is diagonal

	$\mathbf{h}^{\mp}_{a}\gamma$	$\mathbf{h}^{\mp}_{a}\mathbf{Z}$	$\mathbf{h}^{\mp}_{b}\gamma$	$\mathbf{h}^{\mp}_{b}\mathbf{Z}$
$\mathbf{h}^{\pm}_{a}$	✓	✓	–	–
$\mathbf{h}^{\pm}_{b}$	–	–	✓	✓

	$\mathbf{h}_a\mathbf{h}_a$	$\mathbf{h}_a\mathbf{h}_b$	$\mathbf{h}_a\mathbf{h}_c$	$\mathbf{h}^{\pm}_{a}\mathbf{h}^{\mp}_{a}$	$\mathbf{h}^{\pm}_{b}\mathbf{h}^{\mp}_{b}$	$\mathbf{h}^{\pm}_{a}\mathbf{h}^{\mp}_{b}$	$\chi_a\chi_a$	$\chi_b\chi_b$	$\chi_a\chi_b$
$\mathbf{h}_a$	–	✓	✓	–	–	✓	–	–	✓
$\mathbf{h}_b$	✓	–	–	✓	✓	–	✓	✓	–
$\mathbf{h}_c$	✓	–	–	✓	✓	–	✓	✓	–

Table 2.2: *Other 3-point vertices. A checkmark indicates that the vertex exists.*

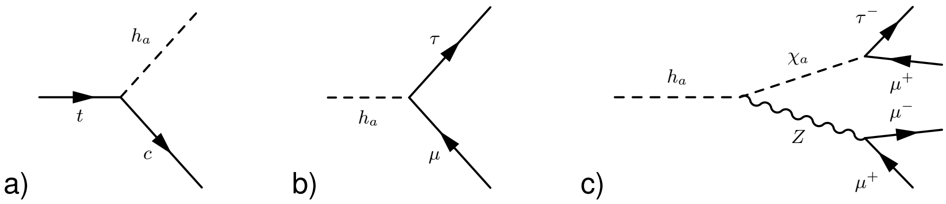

Figure 2.2: *Feynman graphs for dominant sources of h_a production and decays which might be relevant at the LHC.*

being generated by a type-II seesaw mechanism, the large mixing angles in the lepton sector survive. There are two generic textures of Yukawa couplings in our model [21, 22]:

$$Y_a = \begin{pmatrix} 0 & 0 & Y_{13} \\ 0 & 0 & Y_{23} \\ Y_{31} & Y_{32} & 0 \end{pmatrix}, \quad Y_{b,c} = \begin{pmatrix} Y_{11} & Y_{12} & 0 \\ Y_{21} & Y_{22} & 0 \\ 0 & 0 & Y_{33} \end{pmatrix}. \tag{2.10}$$

Here Y_a symbolically describes the Yukawa couplings for h_a, χ_a and h^+_a, while $Y_{b,c}$ describe the couplings for h_b, h_c, χ_b and h^+_b, and the pattern holds both for leptons and quarks. The off-diagonal couplings in $Y_{b,c}$ are numerically small and can be controlled by one free parameter which keeps dangerous FCNC processes under control. The largest off-diagonal coupling in Y_a is $(h_a/\chi_a)ct \sim 0.8$; it leads to viable production channel of h_a via t decays. The next largest couplings are $(h_a/\chi_a)sb \approx 0.02$ and $(h_a/\chi_a)\mu\tau \approx 0.008$. The $\chi_a\mu\tau$ coupling leads to an interesting decay channel that can lead to observable signatures at the LHC.

2.4 How to search for h_a at the LHC?

If kinematically allowed, h_a can be produced e.g. through $t \to h_a c$ [Fig. 2.2(a)]. After that, if $m_{h_a} < m_{\chi_a}$, h_a decays dominantly into b and s quarks, or into τ and μ [see Fig. 2.2(b)]. The branching ratio (BR) for $t \to h_a c$ is $0.17(0.06)$ for $m_{h_a} = 130(150)$ GeV. Then $h_a \to \mu\tau$ occurs with a BR of 10% and $h_a \to bs$ with 90%.

We stress on a spectacular channel that opens up when $h_a \to \chi_a Z$ is kinematically accessible [Fig. 2.2(c)]. The corresponding BR is almost 100% since gauge couplings dominate over

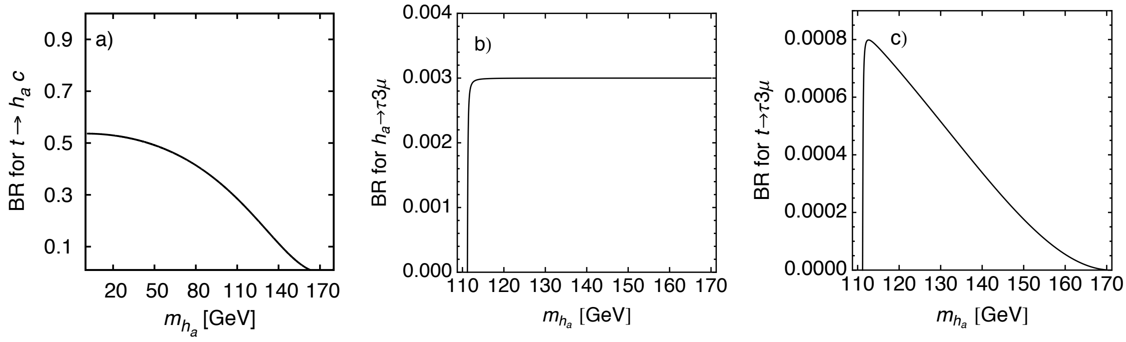

Figure 2.3: *Different branching ratios involving the production and decay of h_a. In all cases, $m_{\chi_a} = 20$ GeV is assumed.*

the light fermion Yukawa couplings. Then $\chi_a \to \tau\mu$ proceeds with a BR of 10%, and $Z \to \mu\mu$ occurs with a BR of 3%. If two h_a are produced from $t\bar{t}$ pairs, this could lead to a characteristic signal with up to six muons with the taus used as tags. The relevant BRs are plotted in Figs. 2.3(a)–(c). Throughout we have assumed that $m_{\chi_a} = 20$ GeV.

2.5 Conclusions and outlook

We have analyzed the complete scalar/pseudoscalar sector of an S_3 flavor model. We simultaneously handle three CP-even, two CP-odd and two sets of charged scalar particles. We followed a novel technique of potential minimization which allowed to us to explore the parameter space better. The scalar h_b mimicks the standard Higgs-like object weighing around 125 GeV, while h_a and χ_a evade conventional collider searches at LEP/Tevatron/LHC and hence can be rather light. The other scalars/pseudoscalars can stay beyond the current LHC reach (e.g., 550 GeV). We stressed on a promising channel for h_a search at LHC involving up to six muons in the final state to be searched with the tau tags. We urge our experimental colleagues to look for this channel.

Bibliography

[1] G. Altarelli and F. Feruglio, Rev.Mod.Phys. **82**, 2701 (2010), arXiv:1002.0211 [hep-ph] .

[2] E. Ma, (2007), arXiv:0705.0327 [hep-ph] .

[3] E. Ma, New J.Phys. **6**, 104 (2004), arXiv:hep-ph/0405152 [hep-ph] .

[4] H. Ishimori, T. Kobayashi, H. Ohki, Y. Shimizu, H. Okada, and M. Tanimoto, Prog.Theor.Phys.Suppl. **183**, 1 (2010), arXiv:1003.3552 [hep-th] .

[5] S. Pakvasa and H. Sugawara, Phys.Lett. **73B**, 61 (1978).

[6] P. V. Dong, H. N. Long, C. H. Nam, and V. V. Vien, Phys.Rev. **D85**, 053001 (2012), arXiv:1111.6360 [hep-ph] .

[7] W. Grimus and L. Lavoura, JHEP **0508**, 013 (2005), arXiv:hep-ph/0504153 [hep-ph] .

[8] P. Harrison and W. Scott, Phys.Lett. **B557**, 76 (2003), arXiv:hep-ph/0302025 [hep-ph] .

[9] E. Ma, Phys.Rev. **D43**, R2761 (1991).

[10] E. Ma, Phys.Rev. **D61**, 033012 (2000), arXiv:hep-ph/9909249 [hep-ph] .

[11] R. N. Mohapatra, A. Perez-Lorenzana, and C. A. de Sousa Pires, Phys.Lett. **B474**, 355 (2000), arXiv:hep-ph/9911395 [hep-ph] .

[12] R. N. Mohapatra, S. Nasri, and H.-B. Yu, Phys.Lett. **B639**, 318 (2006), arXiv:hep-ph/0605020 [hep-ph] .

[13] S. Morisi and M. Picariello, Int.J.Theor.Phys. **45**, 1267 (2006), arXiv:hep-ph/0505113 [hep-ph] .

[14] T. Teshima, Phys.Rev. **D73**, 045019 (2006), arXiv:hep-ph/0509094 [hep-ph] .

[15] T. Teshima, Phys.Rev. **D85**, 105013 (2012), arXiv:1202.4528 [hep-ph] .

[16] Q.-H. Cao, A. Damanik, E. Ma, and D. Wegman, Phys.Rev. **D83**, 093012 (2011), arXiv:1103.0008 [hep-ph] .

[17] S.-L. Chen, M. Frigerio, and E. Ma, Phys.Rev. **D70**, 073008 (2004), arXiv:hep-ph/0404084 [hep-ph] .

[18] D. Meloni, JHEP **1205**, 124 (2012), arXiv:1203.3126 [hep-ph] .

[19] S. Dev, R. R. Gautam, and L. Singh, Phys.Lett. **B708**, 284 (2012), arXiv:1201.3755 [hep-ph] .

[20] S. Zhou, Phys.Lett. **B704**, 291 (2011), arXiv:1106.4808 [hep-ph] .

[21] G. Bhattacharyya, P. Leser, and H. Päs, Phys.Rev. **D83**, 011701 (2011), arXiv:1006.5597 [hep-ph] .

[22] G. Bhattacharyya, P. Leser and H. Päs, Phys. Rev. D **86**, 036009 (2012) arXiv:1206.4202 [hep-ph].

[23] S. L. Glashow and S. Weinberg, Phys.Rev. **D15**, 1958 (1977).

[24] J. Kubo, A. Mondragón, M. Mondragón, and E. Rodríguez-Jáuregui, Prog.Theor.Phys. **109**, 795 (2003), arXiv:hep-ph/0302196 [hep-ph] .

[25] Y. Yamanaka, H. Sugawara, and S. Pakvasa, Phys.Rev. **D25**, 1895 (1982).

[26] J. Kubo, H. Okada, and F. Sakamaki, Phys.Rev. **D70**, 036007 (2004), arXiv:hep-ph/0402089 [hep-ph] .

[27] G. Aad *et al.* [ATLAS Collaboration], Phys. Lett. B **716**, 1 (2012) [arXiv:1207.7214 [hep-ex]].

[28] S. Chatrchyan *et al.* [CMS Collaboration], Phys. Lett. B **716**, 30 (2012) [arXiv:1207.7235 [hep-ex]].